

## Synthesis and the electronic spectra of the first $\beta$ -ketoacylsilanes and their lithium enolates: new insights into hyperconjugation in acylsilanes and their enolates<sup>1,2</sup>

Yitzhak Apeloig<sup>a,\*</sup>, Ilya Zharov<sup>a</sup>, Dmitry Bravo-Zhivotovskii<sup>a</sup>, Yuri Ovchinnikov<sup>b,\*</sup>,  
Yuri Struchkov<sup>b</sup>

<sup>a</sup> Department of Chemistry, Technion–Israel Institute of Technology, Haifa 32000, Israel

<sup>b</sup> INEOS, Vavilov Street 28, Moscow B-334, 117813, Russia

Received 19 December 1994

### Abstract

The reaction of tetramethyl-1,3-cyclobutanedione (1) with  $R_2SiLi$  ( $R = Me, Si$  or  $Et$ ) and  $Et_3GeLi$  results in the opening of the cyclobutanedione ring to give the corresponding  $\beta$ -ketoacylsilane lithium enolates **2a–2c**, which after aqueous work-up gave the first known  $\beta$ -ketoacylsilanes **3a** and **3b** and  $\beta$ -ketoacylgermane **3c**. The first X-ray structure of a  $\beta$ -ketoacylsilane, that of lithium enolate **2a**, is reported and discussed. The UV–visible spectra of the lithium enolates **2** exhibits two new transitions: one absorption is “red” shifted and the other is “blue” shifted (each by about 40–50 nm) relative to the absorptions of the corresponding  $\beta$ -ketoacylsilanes. Ab initio molecular orbital calculations show that the “red-shifted” transitions result from the presence of a low-lying Rydberg-type antibonding O–Li orbital, while the “blue-shifted” transition results from a weakening (due to  $Li^+$  complexation) of the destabilizing hyperconjugative interactions between the oxygen lone pair ( $n_O$ ) and the  $\sigma_{C-Si}$  orbital, which leads to a lowering of the energy of the filled ( $n_O-\sigma_{C-Si}$ ) orbital (relative to its energy in the acylsilanes), and thus to a higher ( $n_O-\sigma_{C-Si}$ )  $\rightarrow \pi^*_{C=O}$  excitation energy than in the corresponding acylsilanes.

**Keywords:** Silicon; UV spectra; Hyperconjugation; Crystal structure; Lithium enolate; MO calculations

### 1. Introduction

Acylsilanes constitute a very interesting class of organosilicon compounds [1,2], as they are useful synthons in organic synthesis [1–3] and show unique spectroscopic properties [1–4]. Acylsilanes are usually colored [3], in contrast with the analogous alkyl ketones, suggesting that they might exhibit interesting photochemistry, as was indeed found [4–6]. One of the most striking reactions of acylsilanes is the photochemical 1,3-rearrangement of the silyl group from silicon to oxygen, leading to silenes which contain a Si=C double bond [5]. The first “indefinitely” stable silene was synthesized through this photochemical conversion [6].

The unusual spectroscopic properties of acylsilanes have been studied intensively ever since they were first prepared [3], and several theoretical models were proposed to account for the fact that acylsilanes absorb at a much longer wavelength than do the analogous alkyl ketones [7–14]. The current generally accepted explanation for the unusual spectra of acylsilanes is based on the concept of strong mixing between the lone-pair electrons on the carbonyl oxygen atom and the C–Si bond [11–14]. The geometry of the excited state [13] and the dative type of bonding between the silyl and the carbonyl groups [14] were also suggested to be important factors.

In this paper we report the synthesis and the UV–visible spectra of the first  $\beta$ -ketoacylsilanes and  $\beta$ -ketoacylgermanes and their lithium enolates. The UV–visible spectra of these novel compounds, and particularly these of their lithium enolates, shed new light on the intramolecular orbital interactions in acylsilanes.

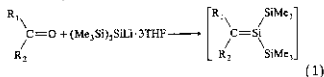
<sup>1</sup> Dedicated to Professor Hideki Sakurai, a pioneer in the field of organosilicon chemistry, on the occasion of his retirement from Tohoku University.

<sup>2</sup> Corresponding authors.

## 2. Results and discussion

### 2.1. Synthesis

We found recently [15a] that  $(\text{Me}_3\text{Si})_3\text{SiLi} \cdot 3\text{THF}$  (THF = tetrahydrofuran) reacts with ketones to produce the corresponding transient silenes:



While exploring the scope of the reaction we treated  $(\text{Me}_3\text{Si})_3\text{SiLi} \cdot 3\text{THF}$  with tetramethyl-1,3-cyclobutanedione (**1**). In contrast with that of other ketones, reaction of **1** with 1 molar equivalent of  $(\text{Me}_3\text{Si})_3\text{SiLi} \cdot 3\text{THF}$  did not lead to the corresponding silene, but to the cleavage of the cyclobutanedione ring to give a 47% yield of the lithium enolate **2a** (Scheme 1). The use of a twofold excess of  $(\text{Me}_3\text{Si})_3\text{SiLi} \cdot 3\text{THF}$  did not change the course of the reaction (or the yield) and only mono-addition occurred. Aqueous work-up gave the first known  $\beta$ -ketoacylsilane **3a**. Reaction of **2a** with  $\text{Me}_3\text{SiCl}$  gave the silyl enol ether **4a** (Scheme 1).

In order to explore the generality of this ring-opening reaction for synthesizing other  $\beta$ -ketoacylsilanes or  $\beta$ -ketoacylgermanes (also previously unknown), we also treated **1** with triethylsilyllithium and triethylgermyllithium (Scheme 1). As in the reaction of **1** with  $(\text{Me}_3\text{Si})_3\text{SiLi} \cdot 3\text{THF}$  in these cases the major products were again the expected ring-opened products, i.e. **2b** and **2c** respectively, producing after aqueous work-up the corresponding  $\beta$ -ketoacylsilane **3b** and  $\beta$ -ketoacylgermane **3c** (Scheme 1). In these cases, ketones of

type **7** were also observed among the products and, when 2 molar equivalents of the lithium reagents were used, the yield of **7** increased at the expense of products **3**. The formation of **7** can be described formally as resulting from the attack of  $\text{RLi}$  at the tertiary carbon of **1** (not at the carbonyl group as in Scheme 1), followed by decarbonylation, as shown in Scheme 2. The mechanism of the interesting reaction leading to the formation of **7** was not elucidated further.

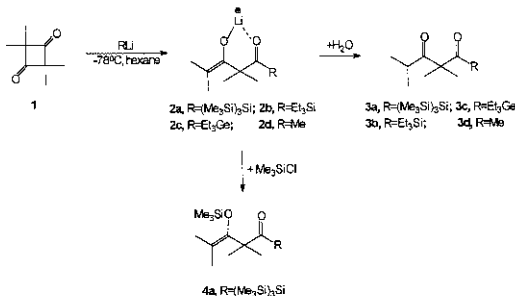
Analogous ring cleavage reactions were reported for the reactions of **1** with a variety of nucleophiles [16] but the reactions with alkyl lithium or Grignard reagents were not studied previously. We have now found that with methyl lithium in hexane **1** again undergoes the analogous ring cleavage to give **2d**, leading after aqueous work-up to the 1,3-diketone **3d** (Scheme 1).

The lithium silaacylenolate **2a** was isolated from its hexane solution as orange prismatic crystals suitable for X-ray analysis.

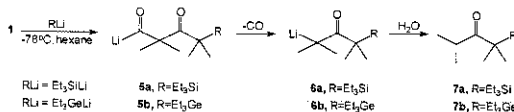
### 2.2. Crystal structure of **2a**

Crystallographic data for **2a** are shown in Table 1, with bond lengths in Table 2 and bond angles in Table 3. A PLUTO drawing of the structure of **2a** (giving the atom numbering) is shown in Fig. 1.

The crystal **2a** is a tetramer, with four lithium atoms and four oxygen atoms occupying pairwise the corners of a cube, with  $\text{Li}-\text{O}$  distances of about 1.9–2.1 Å, as shown in Fig. 2(a). A closer view of the cubane framework of the tetramer, which also shows the numbering of the core atoms, is displayed in Fig. 2(b). Cavities in the crystal packing of the **2a** tetramers are filled by two crystallographically independent hexane molecules.



Scheme 1. Reactions of 2,2,4,4-tetramethyl-1,3-cyclobutanedione (**1**) with various organolithium reagents.



Scheme 2. A possible reaction mechanism for the formation of 7 in the reaction of tetramethyl-1,3-cyclobutanedione (1) with triethylsilyllithium.

Table 1  
Atom coordinates and temperature factors in the structure of 2a

Atom	x ( $\times 10^{-4}$ )	y ( $\times 10^{-4}$ )	z ( $\times 10^{-4}$ )	U ( $\times 10^{-3} \text{ \AA}^2$ )
Si(1)	2200.8(11)	4081.0(31)	404.0(5)	36(1) <sup>a</sup>
Si(2)	2507.2(11)	3231.2(12)	-31.3(6)	46(1) <sup>a</sup>
Si(3)	2974.5(12)	4066.9(12)	916.9(6)	44(1) <sup>a</sup>
Si(4)	2222.5(12)	5141.4(12)	101.3(6)	51(1) <sup>a</sup>
Li(1)	677(6)	2549(6)	985(3)	36(4) <sup>a</sup>
O(1)	1429(2)	3096(3)	703(1)	31(2) <sup>a</sup>
O(2)	-67(2)	3231(2)	965(1)	28(2) <sup>a</sup>
C(1)	1392(4)	3698(4)	640(2)	32(3) <sup>a</sup>
C(2)	781(4)	4062(4)	782(2)	30(3) <sup>a</sup>
C(3)	880(5)	4116(5)	1230(2)	37(3) <sup>a</sup>
C(4)	705(5)	4775(5)	637(3)	42(4) <sup>a</sup>
C(5)	180(3)	3625(3)	680(2)	27(3) <sup>a</sup>
C(6)	-76(4)	3562(4)	317(2)	37(3) <sup>a</sup>
C(7)	-674(4)	3153(5)	242(2)	37(3) <sup>a</sup>
C(8)	238(3)	3869(6)	-43(2)	49(4) <sup>a</sup>
C(9)	1809(6)	3033(8)	-367(3)	63(5) <sup>a</sup>
C(10)	3234(6)	3498(8)	-335(3)	68(5) <sup>a</sup>
C(11)	2743(7)	2468(6)	235(3)	63(5) <sup>a</sup>
C(12)	2952(7)	4854(6)	1194(3)	64(5) <sup>a</sup>
C(13)	2791(6)	3353(5)	1246(3)	50(4) <sup>a</sup>
C(14)	3826(6)	3957(7)	722(4)	66(5) <sup>a</sup>
C(15)	3083(8)	5250(9)	-71(7)	105(7) <sup>a</sup>
C(16)	1646(6)	5189(6)	-321(3)	66(5) <sup>a</sup>
C(17)	2048(8)	5868(5)	425(3)	61(5) <sup>a</sup>
C(18) <sup>bc</sup>	5000	2500	1432(6)	141(7)
C(19) <sup>b</sup>	5437(9)	2850(9)	1125(6)	225(9)
C(20) <sup>b</sup>	5903(9)	3300(9)	1352(5)	182(7)
C(21) <sup>bc</sup>	6263(11)	3707(12)	1040(6)	107(8)
C(22) <sup>c</sup>	5414(30)	5440(33)	1251(15)	80(14)
C(23) <sup>d</sup>	4973(49)	5863(57)	832(37)	188(35)
C(24) <sup>d</sup>	4461(26)	6727(27)	305(17)	109(16)
C(25) <sup>d</sup>	4687(39)	6302(49)	262(2)	129(30)
C(26) <sup>d</sup>	5343(25)	5282(27)	825(14)	88(14)
C(27) <sup>d</sup>	4529(25)	6632(31)	-37(15)	95(17)
C(28) <sup>d</sup>	4765(48)	6300(48)	1073(26)	183(33)
C(29) <sup>d</sup>	5637(30)	5842(34)	1374(17)	105(19)
C(30) <sup>d</sup>	5023(29)	5414(27)	1152(15)	82(15)
C(31) <sup>d</sup>	5547(35)	4990(39)	1082(22)	149(24)
C(32) <sup>d</sup>	4768(30)	7172(32)	213(17)	143(21)
C(33) <sup>d</sup>	4746(29)	6347(35)	628(18)	125(19)
C(34) <sup>d</sup>	4893(34)	5691(40)	166(21)	160(24)
C(35) <sup>d</sup>	5260(63)	5973(63)	1158(36)	209(37)
C(36) <sup>d</sup>	4897(29)	5811(32)	600(21)	113(20)

<sup>a</sup> Equivalent isotropic U defined as one third of the trace of the orthogonalized  $U_{ij}$  tensor

<sup>b</sup> The first solvent molecule.

<sup>c</sup> The site occupation 0.5.

<sup>d</sup> The second solvent molecule; all the occupation factors are 0.25.

The indexes (a) and (b) indicate the symmetry transformations  $-x$ ,  $0.5 - y$ ,  $z$  and  $-0.25 + y$ ,  $0.25 - x$ ,  $0.25 - z$ .

Using a simple electrostatic model Amstutz et al. [17] calculated an energy gain of about  $300 \text{ kcal mol}^{-1}$  upon formation of a Li enolate tetramer from four isolated monomers. Since the geometry of the  $(\text{LiO})_4$  cubane framework of 2a (Fig. 2(b) and Tables 2 and 3) is very similar to that considered by Amstutz et al. [17] or that of other lithium enolates [18,19], a similar stabilization would be expected to result from the tetramerization of 2a. Thus, like most other Li enolates [19], 2a probably also exists as a tetramer in non-polar solvents.

In known acylsilanes the Si–C(O) bond length is in the range 1.90–1.94 Å [1,20]. When the electrons of the C=O bond are delocalized (e.g. when N or O substituents are bonded to the C=O group) the Si–C(O) bond is, as expected, shorter (1.905–1.925 Å [20]) than in simple alkyl acylsilanes (1.929–1.940 Å [21]). All these Si–C bond lengths are significantly longer than the typical Si–C(sp<sup>3</sup>) bond length of 1.87 Å [22]. The Si–C(O) bond length in the enolate 2a of 1.976 Å is significantly longer than that in acylsilanes, and this additional elongation can be attributed to the coordination of the carbonyl group to Li<sup>+</sup>. Coordination to Li<sup>+</sup> increases the positive charge on the carbonyl carbon atom and consequently increases the electrostatic repulsion between it and the positively charged silicon (see below) [23], thus elongating the Si–C(O) bond distance.

Table 2  
Selected bond length (Å) in the tetramer of 2a

Si(1)–Si(2)	2.361(3)	Li(1)–O(1)	2.11(1)
Si(1)–Si(3)	2.363(3)	Li(1)–O(2)	2.03(1)
Si(1)–Si(4)	2.375(3)	Li(1)–O(2a)	1.99(1)
Si(1)–C(1)	1.976(8)	Li(1)–O(2b)	1.91(1)
Si(2)–C(9)	1.87(1)	Li(1)–C(5)	2.61(1)
Si(2)–C(10)	1.88(1)	O(1)–C(1)	1.23(1)
Si(2)–C(11)	1.85(1)	O(2)–C(5)	1.359(8)
Si(3)–C(12)	1.85(1)	C(1)–C(2)	1.51(1)
Si(3)–C(13)	1.87(1)	C(2)–C(3)	1.573(9)
Si(3)–C(14)	1.85(1)	C(2)–C(4)	1.52(1)
Si(4)–C(15)	1.84(2)	C(2)–C(5)	1.53(1)
Si(4)–C(16)	1.87(1)	C(5)–C(6)	1.37(1)
Si(4)–C(17)	1.88(1)	C(6)–C(7)	1.48(1)
		C(6)–C(8)	1.53(1)

The C=O bond length in **2a**, of 1.23(1) Å, is in the usual range for acylsilanes [1,21].

### 2.3. UV-visible spectra

One of the most intriguing properties of acylsilanes is their color. The spectra of the new acylsilanes **3a**, **3b** and **3c** are similar to those of other known acylsilanes [1–4], showing absorption around 370 nm. The additional  $\beta$ -carbonyl group in these acylsilanes has little effect on the transition energy. However, the lithium enolates **2a–2c** exhibit two new interesting absorption maxima: one near 335 nm and the other at 410 nm. The UV-visible absorption spectra of the novel acylsilanes **3a–3c** and the corresponding lithium enolates **2a–2c** are shown in Fig. 3, and relevant data are given in Table 4.

What is the origin of the new absorption bands at 335 nm and 410 nm in the spectra of the lithium enolates? To answer this we need first to discuss briefly the spectra of acylsilanes.

As mentioned above, acylsilanes absorb at about 370 nm whereas the corresponding  $n_{\text{O}} \rightarrow \pi_{\text{C}=\text{O}}$  transition in simple ketones is at about 280 nm [1–4]. Early explanations of this large fall in the excitation energy when silyl groups are attached to the carbonyl carbon focused on the idea that the excited state of acylsilanes is stabilized by participation of d orbitals on silicon and on inductive destabilization of the oxygen lone pairs by the electropositive silicon [7–10]. However, more recent

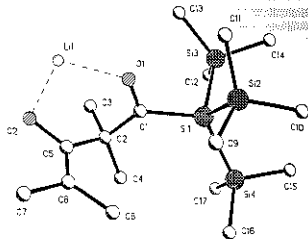


Fig. 1. ORTEP drawing of the structure of **2a** showing atom numbering. Coordination to neighboring Li atoms is shown by broken lines. Hydrogen atoms are omitted for clarity.

photoelectron spectroscopy studies and CNDO/2 calculations [11] have shown that the main reason for the observed shifts is a strong mixing between the in-plane lone-pair orbital on oxygen ( $n_{\text{O}}$ ) and the C–Si  $\sigma$  bond, which pushes the filled antibonding combination of these orbitals (i.e.  $n_{\text{O}}-\sigma_{\text{C}-\text{Si}}$ ) to a higher energy (hyperconjugative destabilization), reducing the gap with the empty  $\pi_{\text{C}=\text{O}}$  orbital [11]. These conclusions were reinforced by ab initio calculations [12a]. Experimental evidence in favor of hyperconjugative  $n_{\text{O}}-\sigma_{\text{C}-\text{Si}}$  destabilization was obtained from the vertical ionization energies of acylsilanes [12b] and from the electrochemical oxidation potentials of  $\beta$ -silyl ethers [12a]. Evidence for stabilization of the lowest vacant orbitals of acylsilanes relative to those of alkylketones was obtained from half-wave reduction potentials of various acylsilanes [12a]. More recent molecular orbital analysis suggested that other contributing factors are the similarity of the vertical and the adiabatic excitation energies of acylsilanes [13] and the dative bonding between the  $R_3\text{Si}$  and the C=O groups [14].

### 2.4. Molecular orbital calculations

In order to interpret the changes in the electronic structure which result from coordination of a lithium cation to acylsilanes we performed molecular orbital ab-initio calculations on the model compounds **8** and **9**. Standard ab-initio methods [24] implemented in the Gaussian 90 series of programs were used [25].

The geometries of the ketones **8** were fully optimized by using analytical gradient techniques [25] and the polarized 6-31G\* basis set [26]. Attempts to optimize fully the structures of the corresponding lithium enolates **9** were unsuccessful. Consequently, the following constraints were introduced in the geometry optimiza-

Table 3  
Selected bond angles (°) in the tetramer of **2a**

Si(2)–Si(1)–Si(3)	107.6(1)	Li(1)–O(1)–C(1)	123.5(6)
Si(2)–Si(1)–Si(4)	111.3(1)	Li(1)–O(2)–C(5)	98.6(5)
Si(3)–Si(1)–Si(4)	109.4(1)	Li(1)–O(2)–Li(1a)	85.5(5)
Si(2)–Si(1)–C(1)	101.4(2)	C(5)–O(2)–Li(1a)	135.2(5)
Si(3)–Si(1)–C(1)	103.0(2)	C(5)–O(2)–Li(1c)	85.0(5)
Si(4)–Si(1)–C(1)	123.2(3)	C(5)–O(2)–Li(1e)	138.6(5)
Si(1)–Si(2)–C(10)	111.0(4)	Li(1a)–O(2)–Li(1c)	86.1(5)
Si(1)–Si(2)–C(10)	110.8(5)	Si(1)–C(1)–O(1)	114.0(5)
Si(1)–Si(2)–C(11)	170.2(4)	Si(1)–C(1)–C(2)	127.9(6)
Si(1)–Si(3)–C(12)	111.4(4)	O(1)–C(1)–C(2)	117.8(6)
Si(1)–Si(3)–C(13)	109.9(4)	C(1)–C(2)–C(3)	104.7(6)
Si(1)–Si(3)–C(14)	109.4(4)	C(1)–C(2)–C(4)	115.3(6)
Si(1)–Si(4)–C(15)	105.5(6)	C(3)–C(2)–C(4)	105.9(6)
Si(1)–Si(4)–C(16)	112.2(4)	C(1)–C(2)–C(5)	106.7(6)
Si(1)–Si(4)–C(17)	115.4(3)	C(3)–C(2)–C(5)	111.6(6)
O(1)–Li(1)–O(2)	99.2(6)	C(4)–C(2)–C(5)	112.5(6)
O(1)–Li(1)–O(2a)	146.6(6)	O(2)–C(5)–C(2)	117.0(5)
O(1)–Li(1)–O(2b)	114.4(6)	O(2)–C(5)–C(6)	118.6(6)
O(2)–Li(1)–O(2a)	94.4(5)	C(2)–C(5)–C(6)	124.1(6)
O(2)–Li(1)–O(2b)	93.6(5)	C(5)–C(6)–C(7)	121.3(7)
O(2a)–Li(1)–O(2b)	94.9(5)	C(5)–C(6)–C(8)	124.1(7)
		C(7)–C(6)–C(8)	114.5(7)

Bond angles C(Me)<sub>3</sub>–Si–C(Me)<sub>3</sub> are 106.1–109.5°. The indexes (a), (b) and (c) indicate the symmetry transformations  $-x, 0.5 - y, z$ ;  $-0.25 + y, 0.25 - x, 0.25 - z$  and  $0.25 - y, 0.25 + x, 0.25 - z$  respectively.

tions of **9a** and **9b**: (i) the O–Li<sup>+</sup> bond length was kept constant at 2.11 Å, the O–Li<sup>+</sup> distance determined in the crystal structure of **2a**; (ii) the C=O–Li<sup>+</sup> bond angle was fixed at 120°; (iii) the LiOCR dihedral angle was kept at 180°.

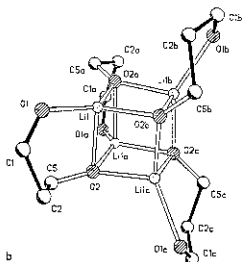
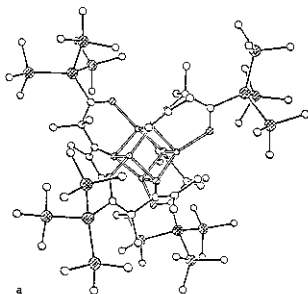
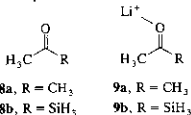


Fig. 2. ORTEP drawings of (a) the **2a** tetramer (hydrogen atoms are omitted for clarity) and (b) the cubane framework of the **2a** tetramer, showing atom numbering. The (a), (b) and (c) symmetry transformations are indicated in the footnote of Table 3. Hydrogen atoms are omitted for clarity. (●, Si; ○, O; □, C; ⊙, Li).

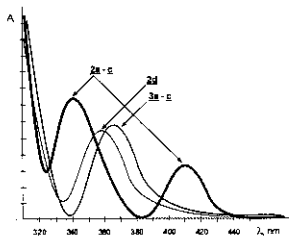


Fig. 3. UV-visible spectra of **2-4**.

The optimized geometries of **8** and the partially optimized geometries of **9** are shown in Fig. 4.

#### 2.4.1. Optimized geometries of the model compounds

The optimized C=O bond lengths in **8a** and **8b** (1.192 Å and 1.197 Å respectively) are similar to those in other ketones and acylsilanes, reflecting the fact that  $\alpha$ -silicon substituents do, not significantly change the carbonyl bond length [1]. The C–Si distance of 1.937 Å in **8b** is in the usual range for simple acylsilanes [1,21,22].

Complexation of the lithium cation to acetone or to acylsilane **8b** leads to a small lengthening (0.022 Å in both cases) of the C=O bond (to 1.214 Å and 1.219 Å respectively). The latter value of 1.219 Å is in good agreement with the experimental value observed for **2a** (1.226 Å). Complexation of Li<sup>+</sup> to **8b** also leads to a 0.021 Å lengthening of the C–Si bond, to 1.958 Å in **9b**, which falls somewhat short of the value of 1.978 Å observed for **2a**. This lengthening can be interpreted as resulting from the increase in the positive charge on the carbonyl carbon atom due to Li<sup>+</sup> complexation (the calculated positive charge on the carbonyl carbon atom is +0.252 in **8b** and +0.277 in **9b**), which in turn increases the repulsion between the carbonyl group and

Table 4  
UV-visible absorption bands of **2-4**

Compound	$\lambda_1$ (e) (nm)	$\lambda_2$ (e) (nm)
<b>2a</b> , R = (Me <sub>2</sub> Si) <sub>2</sub> Si	334 (207)	416 (99)
<b>2b</b> , R = Et <sub>2</sub> Si	328 (90)	408 (56)
<b>2c</b> , R = Et <sub>1</sub> Ge	347 (213)	406 (51)
<b>2d</b> , R = Me	—	364 (225)
<b>3a</b> , R = (Me <sub>2</sub> Si) <sub>2</sub> Si	374 (64)	—
<b>3b</b> , R = Et <sub>2</sub> Si	362 (76)	—
<b>3c</b> , R = Et <sub>1</sub> Ge	372 (46)	—
<b>3d</b> , R = Me	270 (15)	—
<b>4a</b> , R = (Me <sub>2</sub> Si) <sub>2</sub> Si	366 (49)	—

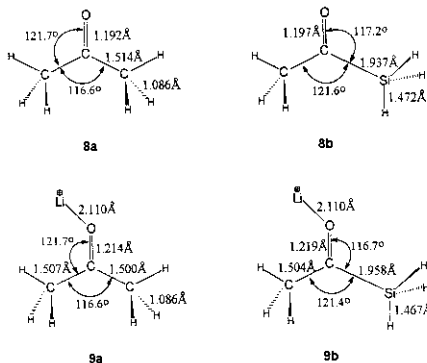
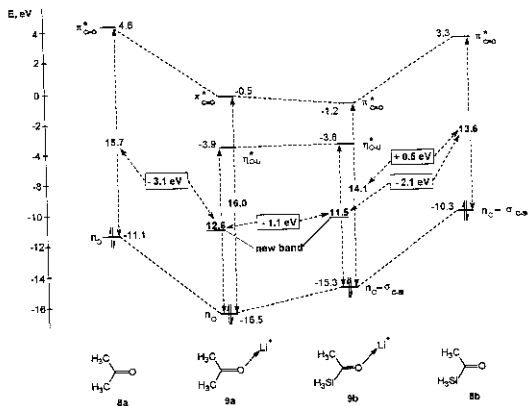


Fig. 4. Optimized geometries (6-31G\*) of the model compounds 8a, 8b, 9a and 9b.

Fig. 5. Highest occupied and lowest unoccupied orbitals (6-31G\*) in acetone (8a), the Li<sup>+</sup>-acetone complex (9a), silacetone (8b) and Li<sup>+</sup>-silacetone complex (9b).

the electropositive silyl group (the charge on Si in **9b** is +0.392), leading to elongation of the C–Si bond. Interestingly, complexation of  $\text{Li}^+$  to acetone leads to the opposite phenomena, the C–C bond being shortened by 0.014 Å.

#### 2.4.2. The electronic structure of the model compounds

The calculated energies of the highest occupied and lowest unoccupied orbitals of silaacetone (**8b**), acetone (**8a**) and the corresponding lithium enolates and the energies of the corresponding electronic transitions are displayed in Fig. 5. The following conclusions may be drawn from the calculations.

(i) Substitution of a methyl group in acetone by a silyl group leads to a substantial reduction of 2.1 eV in the  $n_{\text{O}} \rightarrow \pi_{\text{C}=\text{O}}$  excitation energy (Fig. 5). This is due both (a) to stabilization by 1.3 eV of the  $\pi_{\text{C}=\text{O}}$  orbital in **8b** relative to **8a** and (b) to a destabilization by 0.8 eV of the  $n_{\text{O}}$  orbital in **8b** due to antibonding mixing with the  $\sigma_{\text{C}-\text{Si}}$  orbital, relative to **8a**. This picture is consistent with previous experimental and theoretical analyses of this question [11–14,27]. For example, destabilization of the  $n_{\text{O}}$  orbital in acylsilanes by 1.1 eV and 0.85 eV relative to those in alkyl ketones were found by photoelectron spectroscopy [11] and by vertical ionization energy measurements [12b] respectively. In addition, a polarographic study of acylsilanes revealed an approximately 0.25 eV stabilization of the  $\pi_{\text{C}=\text{O}}$  orbital relative to those for alkyl-substituted ketones [12b]. These experimental results, indicating a reduction in the  $n_{\text{O}} \rightarrow \pi_{\text{C}=\text{O}}$  excitation energy by almost 1 eV, are fully consistent with the differences between the measured UV transition energies for  $\text{BuC(=O)CH}_3$  (4.5 eV;  $\lambda_{\text{max}} = 277$  nm) and those for  $\text{Me}_3\text{SiC(=O)CH}_3$  (3.4 eV;  $\lambda_{\text{max}} = 372$  nm). Comparison with the calculated values for **8b** and **8a** reveals that the calculations significantly overestimate the reduction in the  $n_{\text{O}} \rightarrow \pi_{\text{C}=\text{O}}$  excitation energy which results from the substitution of a methyl group by a silyl group. As the calculated destabilization of the filled  $n_{\text{O}}$  orbital by 0.8 eV in the model acylsilane agrees well with the above-mentioned experimental data [11,12], this must result mostly from an overestimation in the calculated stabilization of the  $\pi_{\text{C}=\text{O}}$  orbitals as a result of substitution, which is not unexpected for virtual orbitals [28].

(ii) The results of the calculations of the effect of  $\text{Li}^+$  coordination to the carbonyl group on the UV–visible spectrum of acetone (**9a**) and of silaacetone (**9b**) are also presented in Fig. 5. Coordination of acetone to  $\text{Li}^+$  leads to a strong but almost identical lowering in the energies of the  $n_{\text{O}}$  orbital (by 5.4 eV) and the  $\pi_{\text{C}=\text{O}}$  orbital (by 5.1 eV), and the  $n_{\text{O}} \rightarrow \pi_{\text{C}=\text{O}}$  transition energy remains almost unchanged. The most interesting feature of the orbital diagram of **9a** is the appearance of a new Rydberg-type vacant orbital ( $\eta_{\text{O}-\text{Li}^+}$ ), not present in acetone, which has mainly 2s ( $\text{Li}^+$ ) character and

which is lower in energy than the  $\pi_{\text{C}=\text{O}}$  orbital (Fig. 5). The calculated excitation energy for the new  $n_{\text{O}} \rightarrow \eta_{\text{O}-\text{Li}^+}$  transition in **9a** is 12.6 eV, smaller by 3.1 eV than the value of 15.7 eV calculated for the  $n_{\text{O}} \rightarrow \pi_{\text{C}=\text{O}}$  transition in acetone. On the basis of these calculations we suggest that the long-wavelength transition at 364 nm observed in the spectrum of the alkyl-enolate **2d** is due to an  $n_{\text{O}} \rightarrow \eta_{\text{O}-\text{Li}^+}$  transition.

(iii) Complexation of  $\text{Li}^+$  to silaacetone has a similar effect to that discussed for acetone (Fig. 5). All the frontier orbitals move to a lower energy as a result of  $\text{Li}^+$  complexation and a new Rydberg-type vacant  $\eta_{\text{O}-\text{Li}^+}$  orbital appears in **9b** at –3.8 eV (Fig. 5). The calculated excitation energy for the new  $n_{\text{O}} \rightarrow \sigma_{\text{C}-\text{Si}} \rightarrow \eta_{\text{O}-\text{Li}^+}$  transition in **9b** is 11.5 eV, smaller by 2.1 eV than the value of 13.6 eV calculated for the  $n_{\text{O}} \rightarrow \sigma_{\text{C}-\text{Si}} \rightarrow \pi_{\text{C}=\text{O}}$  transition in silaacetone. Moreover, in this case the  $n_{\text{O}} \rightarrow \sigma_{\text{C}-\text{Si}} \rightarrow \eta_{\text{O}-\text{Li}^+}$  transition requires 1.1 eV less energy than does the lowest electronic transition in **9a** (12.6 eV) owing to the higher energy of the  $n_{\text{O}} \rightarrow \sigma_{\text{C}-\text{Si}}$  orbital in **9b** relative to the  $n_{\text{O}}$  orbital in **9a**. This prediction of a 1.1 eV (about 100 nm) bathochromic shift in the spectrum of **9b** relative to **9a** is in qualitative agreement with the measured bathochromic (“red”) shifts of about 40 nm observed in the absorption maxima of the silyl enolates **2a–2c** relative to those for the corresponding non-complexed acylsilanes **3a–3c**. Quantitatively the calculations overestimate the bathochromic shift indicating that they probably overestimate the hyperconjugative destabilization of the  $n_{\text{O}} \rightarrow \sigma_{\text{C}-\text{Si}}$  orbital. It is noteworthy that the longest-wavelength absorption in **2a** is red shifted by 8 nm with respect to **2b**, probably owing to the increase in the number of the additional  $\beta$ -silyl substituents in **2a**.

(iv) The overall effect of replacing a methyl group by an  $\text{SiH}_3$  group and complexation to a lithium cation (**9b**) is to induce a substantial decrease of 1.6 eV in the  $n_{\text{O}} \rightarrow \sigma_{\text{C}-\text{Si}} \rightarrow \pi_{\text{C}=\text{O}}$  transition energy relative to the  $n_{\text{O}} \rightarrow \pi_{\text{C}=\text{O}}$  transition in **8a**. However, this effect is smaller than the 2.1 eV difference between these transitions in **8a** and **8b**. Consequently, the  $n_{\text{O}} \rightarrow \sigma_{\text{C}-\text{Si}} \rightarrow \pi_{\text{C}=\text{O}}$  transition in **9b** requires 0.5 eV more energy than in the neutral acylsilane **8b** (Fig. 5). This results from the fact that complexation by  $\text{Li}^+$  reduces the destabilizing hyperconjugation interaction between the  $n_{\text{O}}$  orbital and  $\sigma_{\text{C}-\text{Si}}$  orbital more than it effects the  $\pi_{\text{C}=\text{O}}$  orbital energy. Thus the calculations predict that the  $n_{\text{O}} \rightarrow \sigma_{\text{C}-\text{Si}} \rightarrow \pi_{\text{C}=\text{O}}$  transition in **9b** should be shifted by about 50 nm (0.5 eV). This prediction is in very good agreement with the observed hypsochromic shift of about 40 nm in the UV–visible spectra of the acylsilane enolates **2a–2c** relative to these of the corresponding  $\beta$ -ketoacylsilanes **3a–3c**.

In conclusion, the molecular orbital calculations are in good agreement with the experimentally measured electronic spectra and provide a consistent picture for

understanding the UV–visible spectra of the novel lithium enolates of acylsilanes that we have prepared. We are currently studying the promising photochemistry of the novel  $\beta$ -ketoacylsilanes and their lithium enolates.

### 3. Experimental details

#### 3.1. General comments

NMR spectra were recorded at room temperature in  $\text{CDCl}_3$  or  $\text{C}_6\text{D}_6$  solutions using a Bruker EM-200 or Bruker-400 instrument. Mass spectroscopy (MS) data were obtained with a Finnigan MAT TSO 45 triple-stage quadrupole mass spectrometer. UV–visible spectra were recorded for hexane solution on a Hewlett–Packard 8451A diode array UV–visible spectrophotometer at room temperature using a standard or evacuated 10 mm cell.

#### 3.2. Lithium silacylenolate (2a)

All operations were carried out under vacuum using Schlenk techniques. A solution of ketone I (1.40 g, 0.01 mol) in 20 ml of hexane was added to a solution of 5.2 g (0.015 mol) [29] of  $(\text{Me}_2\text{Si})_2\text{SiLi} \cdot 3\text{THF}$  [30] in 30 ml of hexane cooled to  $-78^\circ\text{C}$ . The red–orange mixture was stirred at  $-78^\circ\text{C}$  for 5 h. Orange crystals of **2a** (2.8 g (47%)) were isolated from the mixture at  $-20^\circ\text{C}$ .  $^1\text{H}$  NMR ( $\text{C}_6\text{D}_6$ ):  $\delta$  0.27 (27H, s,  $(\text{Me}_2\text{Si})_2\text{Si}$ ), 1.23 (6H, s,  $-\text{C}(\text{CH}_3)_2-$ ), 1.75 (3H, s,  $(\text{CH}_3)_2\text{C}=\text{C}$ ), 1.99 (3H, s,  $(\text{CH}_3)_2\text{C}=\text{C}$ ) ppm.  $^{13}\text{C}$  NMR ( $\text{C}_6\text{D}_6$ ):  $\delta$  1.86 ( $\text{Me}_2\text{Si}$ ), 13.73 ( $=\text{CCH}_3$ ), 31.37 ( $\text{C}(\text{O})-\text{C}(\text{CH}_3)_2-\text{C}(\text{O})$ ), 60.30 ( $\text{C}(\text{O})-\text{C}-\text{C}(\text{O})$ ), 91.69 ( $\text{Me}_2\text{C}=\text{C}$ ), 157.91 ( $=\text{C}-\text{OLi}$ ), 260.86 ( $\text{Si}-\text{C}=\text{O}$ ) ppm.  $^{29}\text{Si}$  NMR ( $\text{C}_6\text{D}_6$ ):  $\delta$  -74.75 ( $(\text{Me}_2\text{Si})_2\text{Si}$ ), -11.08 ( $\text{Me}_2\text{Si}$ ). UV–visible spectrum (hexane,  $\epsilon$  values in parentheses): 334 (207), 416 (99) nm.

#### 3.3. X-ray diffraction study of 2a

Crystal data: orange crystals of **2a** are tetragonal; at  $-120^\circ\text{C}$   $a = 20.083(8)$ ,  $c = 34.715(17)$  Å,  $V = 14.000(20)$  Å<sup>3</sup>,  $Z = 16$  ( $\text{C}_{17}\text{H}_{39}\text{O}_2\text{LiSi}_4$ ,  $1.5\text{C}_6\text{H}_{14}$ ),  $d_{\text{calc}} = 0.994$  g  $\text{cm}^{-3}$  and space group  $I4_1/a$ .

Intensities of 4915 unique reflections were measured with a Siemens P3/PC diffractometer (Mo K $\alpha$  radiation; graphite monochromator;  $\theta-2\theta$  scan;  $2\theta_{\text{max}} = 45^\circ$ ). The structure was solved by direct methods and refined by the block-diagonal least-squares technique in an anisotropic approximation for non-hydrogen atoms. Hydrogen atoms of Me groups were located in the difference Fourier maps and refined isotropically. In these maps, several additional electron density peaks corre-

sponding to solvating molecules were found. The molecule lying on the  $\text{C}_2$  symmetry axis is unambiguously identified as hexane. It has a small translational disorder (by one C–C unit) along the chain, and therefore the terminal  $\text{C}(21)$  atom is refined with an occupation factor of 0.5. The second solvating molecule has a greater disorder and an adequate model for its positions could not be found. All atoms of the solvating molecules were refined isotropically. The final values of discrepancy factors are  $R = 0.072$  and  $R_w = 0.066$  for 2313 reflections with  $I > 2\sigma(I)$ . All the calculations were performed using the SHELXTL programs [31]. Atomic coordinates and thermal parameters are given in Table 1, and selected bond lengths and angles in Tables 2 and 3. Tables of hydrogen atom coordinates and thermal parameters, and complete lists of bond length and angles will be deposited at the Cambridge Crystallographic Data Centre.

#### 3.4. 1-Tris(trimethylsilyl)silyl-2,2,4-trimethylheptane-1,3-dione (3a)

Water was added to a hexane solution of **2a** and the organic fraction was separated, washed with 10 ml of water, dried, then the solvent was evaporated to give the crude **3a**, which was further purified by column chromatography on silica gel with a 10:1 hexane–ether mixture as eluent.

$^1\text{H}$  NMR ( $\text{C}_6\text{D}_6$ ):  $\delta$  0.30 (27H, s,  $(\text{Me}_2\text{Si})_2\text{Si}$ ), 0.99 (6H, d,  $(\text{CH}_3)_2\text{CH}$ ,  $^3J_{\text{HH}} = 4$  Hz), 1.28 (6H, s,  $-\text{C}(\text{CH}_3)_2-$ ), 2.73 (1H, spt,  $(\text{CH}_3)_2\text{CH}$ ,  $^3J_{\text{HH}} = 4$  Hz) ppm.  $^{13}\text{C}$  NMR ( $\text{C}_6\text{D}_6$ ):  $\delta$  1.31 ( $\text{Me}_2\text{Si}$ ), 19.42 ( $(\text{CH}_3)_2\text{CH}$ ), 20.42 ( $\text{C}(\text{O})-\text{C}(\text{CH}_3)_2-\text{C}(\text{O})$ ), 36.19 ( $(\text{CH}_3)_2\text{CH}$ ), 67.61 ( $\text{C}(\text{O})-\text{C}-\text{C}(\text{O})$ ), 212.72 ( $\text{C}-\text{C}=\text{O}$ ), 224.81 ( $\text{Si}-\text{C}=\text{O}$ ) ppm.  $^{29}\text{Si}$  NMR ( $\text{C}_6\text{D}_6$ ):  $\delta$  -71.74 ( $(\text{Me}_2\text{Si})_2\text{Si}$ ), -11.84 ( $\text{Me}_2\text{Si}$ ) ppm. MS (CI, relative intensity):  $m/e$  368 ( $\text{M}^+$ , 10), 373 ( $\text{M}^+ - \text{Me}$ , 80), 345 ( $\text{M}^+ - \text{Pr}$ , 85). MS (electron impact (EI)):  $m/e$  373, 1919 ( $\text{M}^+ - \text{Me}$ ) ( $\text{C}_{16}\text{H}_{31}\text{O}_2\text{Si}_4$ , requires 373.1924). UV–visible spectrum (hexane,  $\epsilon$  values in parentheses): 262 (418), 374 (64) nm.

#### 3.5. 1-Tris(trimethylsilyl)silyl-2,2,4-trimethyl-3-trimethylsilyloxy-3-pentene-1-one (4a)

Trimethylchlorosilane was added to a hexane solution of **2a** and work-up as with **3a** was carried out yielding the silyl enol ether **4a**, which could be purified by column chromatography (as with **3a**).

$^1\text{H}$  NMR ( $\text{C}_6\text{D}_6$ ):  $\delta$  0.15 (9H, s,  $\text{OSiMe}_3$ ), 0.31 (27H, s,  $(\text{Me}_2\text{Si})_2\text{Si}$ ), 1.17 (6H, s,  $\text{C}(\text{CH}_3)_2$ ), 1.45 (3H, s,  $(\text{CH}_3)_2\text{C}=\text{C}$ ), 1.57 (3H, s,  $(\text{CH}_3)_2\text{C}=\text{C}$ ) ppm.  $^{13}\text{C}$  NMR ( $\text{C}_6\text{D}_6$ ):  $\delta$  0.65 ( $\text{OSiMe}_3$ ), 1.48 ( $\text{Me}_2\text{Si}$ ), 13.77 ( $=\text{CCH}_3$ ), 22.73 ( $\text{C}(\text{O})-\text{C}(\text{CH}_3)_2-\text{C}(\text{O})$ ), 80.81 ( $\text{C}(\text{O})-\text{C}-\text{C}(\text{O})$ ), 112.16 ( $\text{Me}_2\text{C}=\text{C}$ ), 143.89 ( $=\text{C}-\text{OSiMe}_3$ ), 239.80 ( $\text{Si}-\text{C}=\text{O}$ ) ppm.  $^{29}\text{Si}$  NMR ( $\text{C}_6\text{D}_6$ ):  $\delta$

–76.50 ((Me<sub>3</sub>Si)<sub>3</sub>Si), –11.88 (Me<sub>3</sub>Si), 15.72 (OSiMe<sub>3</sub>) ppm. MS (CI, relative intensity): *m/e* 461 ([M + 1]<sup>+</sup>, 15), 445 (M<sup>+</sup> – Me, 75), 389 (M<sup>+</sup> – OSiMe<sub>3</sub>, 100). MS (EI): *m/e* 445.1759 (C<sub>10</sub>H<sub>40</sub>O<sub>2</sub>Si<sub>3</sub> requires 445.1775). UV-visible spectrum (hexane,  $\epsilon$  value in parentheses): 366 (49) nm.

### 3.6. Lithium acylsilaenolates **2b** and **2c**

Ketone **1** (2.1 g, 0.015 mol) in 20 ml of hexane was added under vacuum to a solution of 0.016 mol of Et<sub>3</sub>MLi (M = Si or Ge) [32] in 30 ml of hexane cooled to –78°C. The yellow reaction mixtures were stirred for 5 h at –78°C. The UV-visible spectrum of the hexane solutions of the enolates **2b** and **2c** revealed the following transitions (hexane,  $\epsilon$  values in parentheses): 328 (90), 408 (56) nm for **2b** and 347 (213), 406 (51) nm for **2c**. After aqueous work-up the crude oily products **3b** and **3c** were obtained.

### 3.7. 1-Triethylsilyl-2,2,4-trimethylpentane-1,3-dione (**3b**)

(2.4 g (63%)) was purified by column chromatography on silica gel with a 10:1 hexane–ether mixture as eluent.

<sup>1</sup>H NMR (CDCl<sub>3</sub>):  $\delta$  0.67, 0.71, 0.74 (9H, t, CH<sub>3</sub> of Et<sub>3</sub>Si); 0.87, 0.89, 0.94, 0.97, 1.01 (18H, m, CH<sub>2</sub> of Et<sub>3</sub>Si + (CH<sub>3</sub>)<sub>2</sub>CH); 1.26 (6H, s, C(CH<sub>3</sub>)<sub>2</sub>); 2.83 (1H, spt, (CH<sub>3</sub>)<sub>2</sub>CH, <sup>3</sup>J<sub>HH</sub> = 4 Hz) ppm. <sup>13</sup>C NMR (CDCl<sub>3</sub>):  $\delta$  3.56, 6.13, 6.64 (Et<sub>3</sub>Si), 19.73 ((CH<sub>3</sub>)<sub>2</sub>CH), 23.15 (C(O)–C(CH<sub>3</sub>)<sub>2</sub>–C(O)), 36.16 ((CH<sub>3</sub>)<sub>2</sub>CH), 66.15 (C(O)–C–C(O)), 216.01 (C–C=O), 244.46 (Si–C=O) ppm. MS (CI, relative intensity): *m/e* 257 ([M + 1]<sup>+</sup>, 3), 241 (M<sup>+</sup> – Me, 75), 228 (M<sup>+</sup> – Pr, 85). MS (EI): *m/e* 228.1919 (M<sup>+</sup> – CO) (C<sub>15</sub>H<sub>28</sub>OSi requires 228.1920). UV-visible spectrum (hexane,  $\epsilon$  values in parentheses): 302 (198), 362 (76) nm.

### 3.8. 1-Triethylgermyl-2,2,4-trimethylpentane-1,3-dione (**3c**)

(1.7 g (45%)) was purified by column chromatography on silica gel with a 10:1 hexane–ether mixture as eluent.

**3c**: <sup>1</sup>H NMR (CDCl<sub>3</sub>):  $\delta$  0.95–1.05 (21H, br m, Et<sub>3</sub>Si + (CH<sub>3</sub>)<sub>2</sub>CH); 1.26 (6H, s, C(CH<sub>3</sub>)<sub>2</sub>); 2.81 (1H, spt, (CH<sub>3</sub>)<sub>2</sub>CH) ppm. <sup>13</sup>C NMR (CDCl<sub>3</sub>):  $\delta$  5.50, 7.55 (Et<sub>3</sub>Si), 19.21 ((CH<sub>3</sub>)<sub>2</sub>CH), 21.97 (C(O)–C(CH<sub>3</sub>)<sub>2</sub>–C(O)), 35.75 ((CH<sub>3</sub>)<sub>2</sub>CH), 66.47 (C(O)–C–C(O)), 213.68 (C–C=O), 240.64 (Si–C=O) ppm. MS (EI, relative intensity): *m/e* 301 ([M – 1]<sup>+</sup>, 3), 287 (M<sup>+</sup> – Me, 70), 274 (M<sup>+</sup> – Et, 100), 259 (M<sup>+</sup> – Pr, 85). UV-visible spectrum (hexane,  $\epsilon$  values in parentheses): 298 (260), 372 (46) nm.

### 3.9. 2,4,4-Trimethyl-4-triethylsilylbutane-3-one (**7a**)

This was isolated as a minor product after column chromatography of the crude reaction mixture obtained from the reaction of **1** with Et<sub>3</sub>SiLi and was characterized by its <sup>1</sup>H NMR and MS.

<sup>1</sup>H NMR (CDCl<sub>3</sub>):  $\delta$  0.69, 0.73, 0.77 (9H, t, CH<sub>3</sub> of Et<sub>3</sub>Si); 0.96, 1.00, 1.03, 1.06 (18H, m, CH<sub>2</sub> of Et<sub>3</sub>Si + (CH<sub>3</sub>)<sub>2</sub>CH); 1.30 (6H, s, C(CH<sub>3</sub>)<sub>2</sub>); 3.06 (1H, spt, (CH<sub>3</sub>)<sub>2</sub>CH) ppm. MS (CI, relative intensity): *m/e* 229 ([M + 1]<sup>+</sup>, 15), 200 (M<sup>+</sup> – Et, 85), 185 (M<sup>+</sup> – Pr, 60).

### 3.10. 2,4,4-Trimethyl-4-triethylgermylbutane-3-one (**7b**)

This was isolated as a minor product after column chromatography of crude **3c** and was characterized by its <sup>1</sup>H NMR and MS.

<sup>1</sup>H NMR (CDCl<sub>3</sub>):  $\delta$  0.97–1.10 (21H, br m, Et<sub>3</sub>Si + (CH<sub>3</sub>)<sub>2</sub>CH); 1.30 (6H, s, C(CH<sub>3</sub>)<sub>2</sub>); 3.06 (1H, spt, (CH<sub>3</sub>)<sub>2</sub>CH). MS (EI, relative intensity): *m/e* 273 ([M – 1]<sup>+</sup>, 5), 259 (M<sup>+</sup> – Me, 75), 246 (M<sup>+</sup> – Et, 100), 218 (M<sup>+</sup> – 2Et, 60).

### 3.11. Lithium acetylenolate **2d**

5 ml of a 5% solution of MeLi (0.012 mol) in ether were added at –78°C under vacuum to a solution of 1.40 g (0.01 mol) of **1** in 30 ml of hexane, and the yellow reaction mixture was stirred for 5 h to give the enolate **2d**. A UV-visible spectrum of the resulting solution revealed transition ( $\epsilon$  value in parentheses) at 364 (225) nm. After aqueous work-up and chromatographic purification of the crude product 3,3,5-trimethylhexane-2,4-dione **3d** (1.2g, (77%)) was obtained.

<sup>1</sup>H NMR (CDCl<sub>3</sub>):  $\delta$  0.99, 1.03 (6H, d, (CH<sub>3</sub>)<sub>2</sub>CH); 1.22 (3H, s, CH<sub>3</sub>–C=O); 1.31 (6H, s, C(CH<sub>3</sub>)<sub>2</sub>); 2.85 (1H, spt, (CH<sub>3</sub>)<sub>2</sub>CH, <sup>3</sup>J<sub>HH</sub> = 4 Hz) ppm. <sup>13</sup>C NMR (CDCl<sub>3</sub>):  $\delta$  20.48, 21.84 ((CH<sub>3</sub>)<sub>2</sub>CH), 29.71 (C(O)–C(CH<sub>3</sub>)<sub>2</sub>–C(O)), 36.70 (CH in <sup>1</sup>Pr), 57.80 (CH<sub>3</sub>–C=O), 95.31 (C(O)–C–C(O)), 194.91 (CH<sub>3</sub>–C=O), 213.52 (Pr–C–C=O) ppm. MS (EI, relative intensity): *m/e* 156 (M<sup>+</sup>, 30), 141 (M<sup>+</sup> – Me, 65), 113 (M<sup>+</sup> – Pr, 15). UV-visible spectrum (hexane,  $\epsilon$  value in parentheses): 276 (230) nm.

### Acknowledgments

This research was partially supported by the German–Israel Binational Science Foundation, by the Fund for the Promotion of Research at the Technion and by the G.-D. Ereschik Fund for Practical Research. D.B.-Z. is grateful to the Ministry of Immigrant Absorption, State of Israel, for a scholarship.

## References and notes

- [1] P.C.B. Page, S.S. Klair and S. Rosenthal, *Chem. Soc. Rev.*, 19 (1990) 147.
- [2] (a) A. Ricci and A. Degl'Innocenti, *Synthesis*, (1989) 647; (b) A.G. Brook, in S. Patai and Z. Rappoport (eds.), *The Chemistry of Organic Silicon Compounds*, Wiley, New York, 1989, Part 2, p. 984.
- [3] (a) A.G. Brook, in R. West (ed.), *Advances in Organometallic Chemistry*, Vol. 7, Academic Press, New York, 1968, p. 95; (b) A.G. Brook and R.J. Mauris, *J. Am. Chem. Soc.*, 79 (1957) 971; (c) A.G. Brook, *J. Am. Chem. Soc.*, 79 (1957) 4373.
- [4] J.C. Dalton, in A. Padwa (ed.), *Organic Photochemistry*, Vol. 7, Marcel Dekker, New York, 1985, p. 149.
- [5] G. Raabe and J. Michl, in S. Patai and Z. Rappoport (eds.), *The Chemistry of Organic Silicon Compounds*, Wiley, New York, 1989, Part 2, p. 1015.
- [6] A.G. Brook, J.W. Harris, J. Lennon and M. El Sheikh, *J. Am. Chem. Soc.*, 101 (1979) 83.
- [7] A.G. Brook, M.A. Quigley, G.J.D. Peddie, N.V. Schwartz and C.H. Warner, *J. Am. Chem. Soc.*, 82 (1960) 5102.
- [8] R. West, *J. Organomet. Chem.*, 3 (1965) 314.
- [9] D.F. Harmish and R. West, *Inorg. Chem.*, 2 (1963) 1082.
- [10] K. Yates and F. Agolini, *Can. J. Chem.*, 44 (1966) 2229.
- [11] B.G. Ramsey, A.G. Brook, A.R. Bassindale and H. Bock, *J. Organomet. Chem.*, 74 (1974) C41.
- [12] (a) S. Matsunaga, S. Ise, J. Yoshida, T. Masekawa and T. Murata, *J. Am. Chem. Soc.*, 112 (1990) 1962; (b) H. Bock, H. Alt and H. Seidl, *J. Am. Chem. Soc.*, 91 (1969) 355.
- [13] R.S. Grev and H.F. Schaefer III, *J. Am. Chem. Soc.*, 111 (1989) 6137.
- [14] S. Chimichi and C. Mealli, *J. Mol. Struct.*, 271 (1992) 133.
- [15] (a) D. Bravo-Zhivotovski, V. Braude, A. Stanger, M. Kapon and Y. Apeloig, *Organometallics*, 11 (1992) 2326. For other related reports see (b) J. Ohshita, Y. Masekawa and M. Ishikawa, *Organometallics*, 10 (1991) 3775; (c) J. Ohshita, Y. Masekawa and M. Ishikawa, *Organometallics*, 12 (1993) 876; (d) H. Oehme, R. Wustrack, A. Heine, G.M. Sheldrick and D. Stalke, *J. Organomet. Chem.*, 452 (1993) 33; (e) C. Krespmeyer, H. Reinke and H. Oehme, *Angew. Chem., Int. Edn. Engl.*, 33 (1994) 1615.
- [16] (a) R.H. Hasek, E.U. Elam, J.C. Martin and R.G. Nations, *J. Org. Chem.*, 26 (1961) 700; (b) R.H. Hasek, R.D. Clark and J.H. Chaudet, *J. Org. Chem.*, 26 (1961) 3130.
- [17] R. Amstutz, W.B. Schweizer, D. Seebach and J.D. Dumitz, *Helv. Chim. Acta*, 64 (1981) 2617.
- [18] D. Seebach, R. Amstutz and J.D. Dumitz, *Helv. Chim. Acta*, 64 (1981) 2622.
- [19] D. Seebach, *Angew. Chem., Int. Edn. Engl.*, 27 (1988) 1624.
- [20] (a) S.J. Rettig and Y. Trautner, *Acta Crystallogr., Sect. C*, 44 (1988) 1850; (b) S.J. Al-Juaid, Y. Derouiche and P.B. Hitchcock, P.D. Lickiss and A.G. Brook, *J. Organomet. Chem.*, 404 (1991) 293; (c) Yu.E. Ovchinnikov, V.E. Shklover and Yu.T. Struchkov, *Zh. Strukt. Khim.*, 30 (1989) 130; (d) J.P. Vidal, J.L. Galligne and J. Falguieres, *Acta Crystallogr., Sect. B*, 28 (1972) 3130.
- [21] H.K. Sharma, S.P. Vincent, R. Vicardi, F. Cervantes and K.H. Pannell, *Organometallics*, 9 (1990) 2109.
- [22] (a) F.H. Allen, O. Kennard, D.G. Watson, L. Brammer, A.G. Orpen and R. Taylor, *J. Chem. Soc., Perkin Trans. II*, (1987) S1; (b) W.S. Sheldrick, in S. Patai and Z. Rappoport (eds.), *The Chemistry of Organic Silicon Compounds*, Wiley, New York, 1989, Part 1, p. 227.
- [23] (a) Y. Apeloig, R. Biton and A. Abu-Freih, *J. Am. Chem. Soc.*, 115 (1993) 2522; (b) Y. Apeloig and A. Strager, *J. Am. Chem. Soc.*, 107 (1985) 2806.
- [24] W.J. Hehre, L. Radom, P. v. Schleyer and J.A. Pople, *Ab Initio Molecular Orbital Theory*, Wiley, New York, 1986.
- [25] M.J. Frisch, M. Head-Gordon, G.W. Trucks, J.B. Foresman, H.B. Schlegel, K. Raghavachari, M.A. Robb, J.S. Binkley, C. Gonzalez, D.J. Defrees, D.J. Fox, R.A. Whiteside, R. Seeger, C.F. Melius, J. Baker, R.L. Martin, L.R. Kahn, J.J.P. Stewart, S. Topiol and J.A. Pople, *VAX/VMS version of the gaussian 90 series of programs* Gaussian, Inc., Pittsburg PA, 1990.
- [26] P.C. Hariharan and J.A. Pople, *Theor. Chim. Acta*, 28 (1973) 213.
- [27] E.B. Nadler, Z. Rappoport, D. Arad and Y. Apeloig, *J. Am. Chem. Soc.*, 109 (1987) 7873.
- [28] (a) E. Steiner, *The Determination and Interpretation of Molecular Wave Functions*, Cambridge University Press, Cambridge, 1976, p. 50; (b) T. Clark, *A Handbook of Computational Chemistry*, Wiley, New York, 1985, p. 93-99.
- [29] Experience shows that the use of 1.5 equivalents of  $(Me_3Si)_2SiLi$  give the best yield of the crystalline compounds 2a. However, the yield after hydrolysis is almost the same in the range of one to two equivalents of  $(Me_3Si)_2SiLi$ .
- [30] G. Gutekunst and A.G. Brook, *J. Organomet. Chem.*, 225 (1982) 1.
- [31] W. Robinson and G.M. Sheldrick, SHELX, in N.W. Isaacs and M.R. Taylor (eds.), *Crystallographic Computing Techniques and New Technologies*, Oxford University Press, Oxford, 1988, p. 366.
- [32] (a) E.N. Gladyshev, N.S. Vyasankin, E.A. Fedorova, L.O. Yuntala and G.A. Razuvaev, *J. Organomet. Chem.*, 64 (1974) 307; (b) E.N. Gladyshev, E.A. Fedorova, L.O. Yuntala, G.A. Razuvaev and N.S. Vyasankin, *J. Organomet. Chem.*, 96 (1975) 169.